

How Sedna and family were captured in a close encounter with a solar sibling

Lucie Jílková,^{1*} Simon Portegies Zwart,^{1*} Tjibbaria Pijloo^{1,2} and Michael Hammer³

¹ *Leiden Observatory, Leiden University, PO Box 9513, 2300 RA, Leiden, The Netherlands*

² *Department of Astrophysics/IMAPP, Radboud University, PO Box 9010, 6500 GL Nijmegen, the Netherlands*

³ *Cornell University, 614 Space Sciences Building, Ithaca, NY 14853*

Accepted . Received ; in original form 2015 March 9

ABSTRACT

The discovery of 2012 VP₁₁₃ initiated the debate on the origin of the Sedna family of planetesimals in orbit around the Sun. Sednitos roam the outer regions of the Solar System between the Egeworth–Kuiper belt and the Oort cloud, in extraordinary wide ($a > 150$ au) orbits with a large perihelion distance of $q > 30$ au compared to the Earth’s ($a \equiv 1$ au and eccentricity $e \equiv (1 - q/a) \simeq 0.0167$ or $q \simeq 1$ au). This population is composed of a dozen objects, which we consider a family because they have similar perihelion distance and inclination with respect to the ecliptic $i = 10^\circ\text{--}30^\circ$. They also have similar argument of perihelion $\omega = 340^\circ \pm 55^\circ$. There is no ready explanation for their origin. Here we show that these orbital parameters are typical for a captured population from the planetesimal disk of another star. Using the orbital parameters of the Sednitos we reconstruct the encounter that led to their capture. We conclude that they might have been captured in a near miss with a $1.8 M_\odot$ star that impacted the Sun at $\simeq 340$ au at an inclination with respect to the ecliptic of $17\text{--}34^\circ$ with a relative velocity at infinity of ~ 4.3 km/s. We predict that the Sednitos-region is populated by 930 planetesimals and the inner Oort cloud acquired ~ 440 planetesimals through the same encounter.

Key words: planetary systems – celestial mechanics – minor planets, asteroids: general; individual: Sedna, 2012 VP₁₁₃ – open clusters and associations

1 INTRODUCTION

Upon its discovery 90377 Sedna (Brown et al. 2004) was proposed to originate from the Egeworth–Kuiper belt; a population of rocks in an almost planar disk aligned with the ecliptic and much closer to the Sun ($q = 30\text{--}50$ au) than the Oort cloud. According to this model the violent and rather sudden migration of Uranus and Neptune would have excited the cold Kuiper belt (Brasser et al. 2012). This reorganization of the outer giant planets would have initiated the hot Kuiper belt (Levison et al. 2008) that, due to the long local relaxation time cools, down only very slowly (Punzo et al. 2014). Subsequent chaotic diffusion (Morbidelli et al. 2008), perturbations in the Sun’s birth environment in close flybys (Davies et al. 2014), or more distant encounters could have caused further migration of the Kuiper-belt objects to orbits similar to that of Sedna (Brasser et al. 2012).

Recently, Trujillo & Sheppard (2014) discovered the object 2012 VP₁₁₃, a second member of the Inner Oort

cloud, which they defined as a family of planetesimals with $q \gtrsim 50$ au and $a \approx 150\text{--}1500$ au. They furthermore identified a population of planetesimals between the Egeworth–Kuiper belt and the Oort cloud that share similar orbital elements (see also de la Fuente Marcos & de la Fuente Marcos 2014), namely the large perihelion and semi-major axis ($q > 30$ au and $a > 150$ au, respectively), inclination with respect to the ecliptic ($i = 10\text{--}30^\circ$), and the argument of perihelion ($\omega = 340^\circ \pm 55^\circ$). Currently 13 such objects have been observed in the outer Solar System and it was suggested that their characteristics resulted from a common origin (Trujillo & Sheppard 2014; de la Fuente Marcos & de la Fuente Marcos 2014). Here we consider this group of object a family which we call *Sednitos*.

The perihelion distances of Sedna and 2012 VP₁₁₃ are too large for any Kuiper belt object and their aphelion distances are too short for them to be Oort cloud objects (Brasser & Schwamb 2015). It is therefore hard to explain them as members of either population. In principle chaotic diffusion could cause sufficient internal migration, but at the distance of Sedna the time scale for this process exceeds the age of the Solar System (Sussman & Wisdom 1988). If

* E-mail: jilkova@strw.leidenuniv.nl (LJ); spz@strw.leidenuniv.nl (SPZ)

Sedna stood alone, such an exotic explanation could be satisfactory. However, this cannot explain the entire population of the inner Oort cloud which, when taking selection effects into account, amounts to 430_{-240}^{+400} members brighter than $r = 24.3$ mag (Trujillo & Sheppard 2014).

According to an alternative scenario, Sedna could have been captured from the outer disk of a passing star, as suggested by Morbidelli & Levison (2004) and Kenyon & Bromley (2004). They showed that capturing a planetesimal into a Sedna-like orbit is possible, but they did not carry out a detailed parameter space study. The model of Kenyon & Bromley (2004) could account for at most 10% of the Sednitos and it was tuned at producing the outer edge of the Edgeworth–Kuiper belt at the currently observed 50 au; however, this is inconsistent with the *Nice* model that requires an edge at ~ 35 au (Gomes et al. 2004).

1.1 Argument of perihelion of Sednitos

Sednitos are characterized by a clustered distribution of their observed argument of perihelion ω . The precession period of ω depends on the semi-major axis, eccentricity, and inclination of the precessing orbit. The precession periods for all Sednitos excluding Sedna range from about 40 Myr up to 650 Myr, while Sedna has the longest precession period of about 1.5 Gyr (Trujillo & Sheppard 2014; Brassier et al. 2006; Gomes et al. 2006). Therefore the clustering of ω must have happened relatively recently (less than few Myr ago) or a dynamical mechanism must have been constraining the distribution of ω since it was established. Trujillo & Sheppard (2014) suggested that an outer Solar System perturber of $5\text{--}15 M_{\text{Earth}}$ orbiting the Sun between 200 and 300 au is restricting the Sednitos’ evolution in ω by the Kozai–Lidov mechanism (Kozai 1962; Lidov 1962). Based on further analysis of the Sednitos’ orbital elements, de la Fuente Marcos & de la Fuente Marcos (2014) suggested that at least two planetary-mass trans-Neptunian perturbers exist at approximately 200 au and 250 au.

The perturbing object (possibly more than one object) is assumed to be on a low-inclination almost circular orbit. When, in such configuration, the ratio of semi-major axis with respect to the perturbed objects (i.e. Sednitos) is close to 1, the relative argument of perihelion of the perturbed and perturbing orbits can librate around 0° or 180° due to the Kozai–Lidov mechanism (see the Extended materials of Trujillo & Sheppard 2014, for an example where ω of 2012 VP₁₁₃ librates around $0^\circ \pm 60^\circ$). However, depending on the initial relative inclination and argument of perihelion of the perturbing and perturbed orbits, the argument of perihelion can also circulate (i.e. periodically changing values from -180° to 180°). The libration around 0° will occur if the initial relative ω ranges from -90° to 90° (e.g. Mardling 2007). Therefore, the ω of Sednitos relative to the perturber ($\omega - \omega_{\text{perturber}}$) needs to be constrained at the beginning of the dynamical interaction with the perturber. Brassier et al. (2006) showed that for the Sedna-like orbits produced during the early evolution of the Solar System, when the Sun was still residing in its birth star cluster, preferentially $\omega = 0^\circ$ or 180° . This mechanism could therefore explain the initial clustering of Sednitos’ argument of perihelion, although it is not clear why the orbits initially obtained ω about 0° and not 180° (see also Trujillo & Sheppard 2014). However, as

mentioned above, the efficiency of this formation channel is probably too low to explain an inner Oort cloud population as populous as predicted from the recent observations (Trujillo & Sheppard 2014).

At the same time, Iorio (2014) ruled out the presence of such a super-Earth planet of $2\text{--}15 M_{\text{Earth}}$ with $a \approx 200\text{--}300$ au using the current constraints on the anomalous secular precession of the argument of perihelion of some of the known planets in the Solar System.

Irrespective of the mechanism that preserves the clustering of the argument of perihelion, we present that such clustering is a general characteristic of the population transferred during a stellar encounter. The constrained distribution in ω can then be shepherded by some other process, possibly by an outer perturber as proposed by Trujillo & Sheppard (2014). At the same time, Sedna and 2012 VP₁₁₃ are found in the Parking zone of the Solar System where their semi-major axis and eccentricity have been unaffected once the Sun left its birth cluster (Portegies Zwart & Jilková 2015). We therefore use the current semi-major axis and eccentricity to constrain the encounter that might have introduced the Sednitos into the Solar System.

2 METHODS

The encounter between the Sun and another star, here called Q, with a planetesimal disk can be simulated by integrating the equations of motion of the two stars using a symplectic N -body code. We use *Huayno* (Pelupessy et al. 2012) for this. As long as the two stars are well separated (at least three times the disk size) we integrate the planetesimals using *Sakura* (Gonçalves Ferrari et al. 2014), in which Kepler’s equations are solved in the potential of the two stars using universal variables. In this approach, the planetesimals are represented by zero-mass particles which do not affect each other and neither the motion of the two stars, while the planetesimals themselves are affected by the two stars. Both integrators are coupled via *Bridge* (Fujii et al. 2007), which is an extension of the mixed variable symplectic scheme (Wisdom & Holman 1991) and is used in this context to couple two different dynamical regimes within one self-gravitating system. The coupling of codes is realized using the Astronomical Multi-purpose Software Environment (Portegies Zwart et al. 2013).¹ When the stars move close enough that the planetesimals orbits can no longer be considered Keplerian—i.e. the motion is no longer dominated by Q and both stars have a substantial influence on the orbits—the planetesimals are integrated directly using *Huayno*. We introduce this transition from hybrid to direct integration when the time since the beginning of the encounter equals half of the time for the two stars to reach their closest approach (which always results to a separation of the two stars larger than three times the disk size).

The initial conditions for the encounter are as follows. The distance between the two stars is determined by the condition that the magnitude of the gravitational force from the Sun at the outer edge of Q’s disk equals 10% of Q’s force. We tested that increasing the initial separation does not change

¹ All source code is available at <http://amusecode.org>.

Table 1. Reconstructed encounter parameters for the star that delivered the Sednitos into the Solar System. The first column lists the five parameters of the encounter: M_Q is the mass of the impactor star Q, q_Q the closest approach of the Sun and Q, e_Q the eccentricity of their orbit, i_Q the inclination of the orbital plane with respect to Q’s disk, and ω_Q the argument of periastron. We further give the impact parameter b , the relative velocity at infinity v of the encounter, and the limits for the outer edges for Q’s and Sun’s disk, $r_{\max,Q}$ and $r_{\max,\odot}$, respectively. The orientation of the encounter with respect to the ecliptic is specified by i_{enc} and ω_{enc} . The second column gives the range considered in the Markov chain simulations, followed by the range of parameters that led to a satisfactory solution. The parameters of the preferred encounter are listed in the right most column (we give the constrained range for i_{enc} and ω_{enc} with the individual values used in the presented example in the parenthesis).

parameter	parameter range	viable range	preferred encounter
M_Q	0.2–2.0 M_\odot	1.0–2.0 M_\odot	1.8 M_\odot
q_Q	200–393 au	210–320 au	227 au
e_Q	1.001–4.0	1.9–3.8	2.6
i_Q	0–180°	2–44°	35°
ω_Q	0–180°	0–180°	175°
b	265–2071 au	280–450 au	340 au
v	0.4–6.0 km/s	3.1–5.4 km/s	4.3 km/s
$r_{\max,Q}$		130–200 au	\gtrsim 161 au
$r_{\max,\odot}$			\lesssim 70 au
i_{enc}		0–70°	17–34° (28°)
ω_{enc}		0–360°	154–197° (170°)

the results. In all our calculations we adopted the mass of the Sun of $1 M_\odot$. Planetesimals in Q’s disk have initially planar distribution and their radial distance from Q, r , follows a uniform random distribution, i.e. the surface density profile of Q’s disk $\propto (1/r)$. However, since the planetesimals are represented by zero-mass particles, the surface density profile can be adjusted in post-processing (see Sec. 3). The planetesimals are initially on circular orbits. The inner edge of Q’s disk is 10 au. We set the upper limit on the outer edge of Q’s disk, $r_{\max,Q}$, to 200 au and determine the actual value from the minimal requirement of producing planetesimals in the range of $q = 30$ au to 85 au; we do the same for Sun’s disk, see below.

The encounter between the Sun and Q is characterized by the five parameters (also listed in Tab. 1)—the mass of the encountering star, M_Q , the closest approach of the stars, q_Q , the eccentricity of the orbit, e_Q , the inclination of the encounter plane with respect to Q’s disk, i_Q , and the argument of periastron of the orbit, ω_Q . We have the computer map this parameter space automatically using the affine-invariant, parallel stretch-move algorithm for Markov Chain Monte Carlo (Hastings 1970) with specific optimizations (Goodman & Weare 2010) using `emcee` (Foreman-Mackey et al. 2013).

We run more than 10,000 realizations of possible encounters. Each calculation is performed with up to 20,000 particles (in chunks of 500) in the planetesimal disk until the number of particles captured by the Sun amounts to at least 13 objects with a perihelion distance between $q = 30$ au and 85 au. To account for the observability of orbits with dif-

ferent eccentricities, we weight each particle by the time it spends within 85 au from the Sun measured as a fraction of the orbital period. The weight w is calculated using the mean anomaly at the 85 au from the Sun, $M(85 \text{ au})$,

$$w = \begin{cases} M(85 \text{ au})/\pi & \text{if aphelion} > 85 \text{ au,} \\ 1 & \text{if } 30 \text{ au} < \text{aphelion} < 85 \text{ au.} \end{cases} \quad (1)$$

This weighting favors finding relatively low eccentricity orbits with a small perihelion, as is consistent with how the Sednitos were discovered (Trujillo & Sheppard 2014).

The resulting distribution of the planetesimals in semi-major axis and eccentricity is subsequently compared with the observed dozen Sednitos listed in Table 2 of Trujillo & Sheppard (2014) and Table 1 in de la Fuente Marcos & de la Fuente Marcos (2014) for 2003 SS₄₂₂. The 13 observed Sednitos provide only low-number statistics and we investigate what constraints can we draw based on the limited data. As a first step in the statistical comparison, we perform a consistency analysis between the simulated objects and the observed Sednitos under the hypothesis that the latter is a random sub-sample of the former using multivariate analysis. We calculate the ranking of the Henze statistic (Henze 1988; Koen & Siluyele 2007) using the nearest neighbors and based on 500 randomly pooled data (see Koen & Siluyele 2007, for more detail) and we require the final rank (or the p -value) of the actual data sets to be > 0.05 to consider the samples consistent. In these cases, we measure the separation distance between these two distributions in **the plane of a vs. e** using the Hellinger distance of binned kernel smoothed distributions (Pak & Basu 1998). We use a grid of 20×20 bins scaled on the observed data with a symmetric Gaussian kernel with a relative width (corresponding to the standard deviation) of 0.08. The separation that emerges from this analysis is used as the posterior probability in the Markov Chain Monte Carlo.

3 RESULTS

We identify a region in the encounter 5-dimensional parameter space where the a vs. e distribution of the simulated transferred particles is statistically indistinguishable from the observed distribution. The runs in the viable range gave the Hellinger distance < 0.6 . We further divide the Sednitos a vs. e region into three sections: the inner Oort cloud ($70 \text{ au} < q < 85 \text{ au}$), the region where so far no objects have been observed ($50 \text{ au} < q < 75 \text{ au}$, or $q < 50 \text{ au}$ and $a < 140 \text{ au}$), and the remaining region. The limits of the viable range for individual parameters are listed in Tab. 1. We also select a preferred encounter as a representative example of the viable range. The parameters of the preferred encounter are also listed Tab. 1. The Sednitos’ distribution produced by the preferred encounter compares well with the observed one: the rank of the Henze statistics is 0.5 and the distance between the distributions is ~ 0.5 (here 0 corresponds to identical binned kernel smoothed distributions, while 1 corresponds to distributions with no overlap; see Sec. 2).

After the Markov chain calculation we constrain the orientation of Q’s disk with respect to the ecliptic. While the inclination i_Q and the argument of periastron ω_Q of the orbital plane of the encounter with respect to Q’s disk are

constrained by the Markov chain calculations, the orientation of the orbital plane with respect to the ecliptic is unconstrained. We constrain the orientation using two-sample Kolmogorov–Smirnov test comparing each of the distributions in the argument of perihelion, inclination, and the longitude of the ascending node of the observed and simulated Sednitos. The clustering of inclination and argument of perihelion is a general feature of the transferred population and an orientation of the coordinate system where the simulated distributions are consistent with the observed ones is found for almost all viable encounters. Using a grid with step size of 2° for each of the three Euler angles, we rotate the coordinate system centered on the Sun until p -value > 0.05 for each of the three compared distributions. We derive the inclination i_{enc} and argument of periastron ω_{enc} of the orbit of the encounter with respect to the ecliptic (the longitude of ascending node is a free parameter due to assumed symmetry of the Sun’s disk, see below). This procedure results in the inclination i_{enc} and the argument of perihelion ω_{enc} of the encounter with respect to the ecliptic for individual encounters. These parameters are typically constrained within intervals of $\pm 10^\circ$ and $\pm 20^\circ$, for i_{enc} and ω_{enc} respectively. We summarize the values in Tab. 1 (note that while always constrained within limited intervals for individual encounters, ω_{enc} have values in a wide range, unlike i_{enc}).

After constraining the initial conditions that reproduce the Sednitos we rerun **the preferred encounter** with 100,000 particles in the disk around the encountering star and 100,000 particles around the Sun. The disk of the Sun extends from 1 au to 200 au. Some perturbed planetesimals of such disk are members of a native population of Sednitos; we compare this population with the transferred population below. The results of this calculation are presented in Fig. 1 and Fig. 2. In Fig. 1, we compare the observed Sednitos with the captured planetesimals from our best reconstruction of the encounter. The orbital distributions of the native and captured planetesimals are presented in Fig. 2.

To estimate the number of planetesimals in the captured and perturbed native population of Sednitos, we adopt a surface density profile $\propto r^{-3/2}$ and a mass of $10^{-3} M_\odot$ for both disks. We further assume that 10% of such disks is in the form of Sedna-mass objects (for which we assume $2 \cdot 10^{21}$ kg). In that case the Sun captured a total of ~ 2600 planetesimals, 884 of which accreted within the orbit of Neptune (with $q < 30$ au), but most of these are probably ejected by interacting with the planets. A total of 936 planetesimals are captured in orbits similar to the observed Sednitos ($q = 30\text{--}50$ au or $q = 75\text{--}85$ au and $a > 150$ au), and 441 in region between $q = 50$ au and 75 au. The inner Oort Cloud ($q > 75$ au, $150 \text{ au} < a \lesssim 1,500$ au) acquired 434 planetesimals, which is consistent with estimates of the current population of 430_{-240}^{+400} (Trujillo & Sheppard 2014). This would require the planetesimal disk of the encountering star to extend at least to 161 au, which is a reasonable disk size for a $\sim 1.8 M_\odot$ star (Booth et al. 2013).

If before the encounter the Sun’s disk extended beyond 90 au, some of its planetesimals are perturbed to a and e consistent with those of the observed Sednitos. Assuming the same surface density profile as for Q’s disk, 307 Sun’s planetesimals would be perturbed in orbits similar to the observed Sednitos ($q = 30\text{--}50$ au or $q = 75\text{--}85$ au and $a > 150$ au), 169 planetesimals would be scattered in the inner Oort Cloud

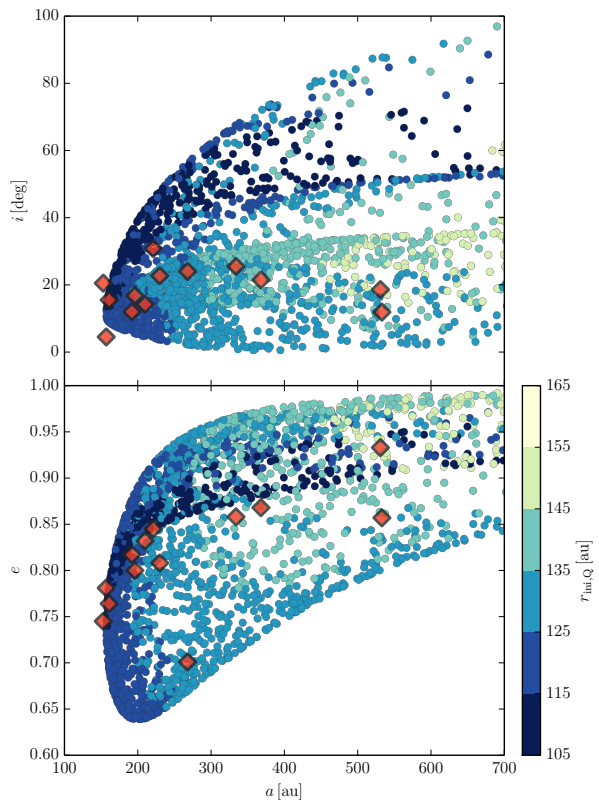


Figure 1. Distribution of captured planetesimals around the Sun from an encounter with star Q using the parameters of the preferred encounter (right most column of Tab. 1). Along the x -axis we present the semi-major axis a of the captured planetesimals. The top panel gives the inclination i along the y -axis, and the bottom panel gives the eccentricity e . The color scale maps the initial radius in Q’s disk, $r_{\text{ini,Q}}$. Note that the simulated particles are not weighted here. The red diamonds give the observed positions of the Sednitos.

($q > 75$ au, $150 \text{ au} < a \lesssim 1,500$ au), and the region between $q = 50$ au and 75 au would be populated by about 319 native scattered planetesimals. We use the best encounter parameters for producing the Sednitos from Tab. 1 to calculate how many of the Sun’s planetesimals would be transferred to the encountering star. If the solar disk extended to 90 au, it would have lost $\sim 2.3\%$ of its planetesimals and $\sim 92\%$ of those were captured by the other star. All the lost planetesimals originate from $a > 70$ au. In the right panel of Fig. 2, we present the distributions of orbital parameters of the Q’s own disk particles, and those of the planetesimals it stole from the Solar System. These captured objects are in rather curious orbits in the outer parts of the disk around the other star. Their inclination is about 14° with respect to Q’s planetesimal disk and their argument of periastron is clustered around $0^\circ \pm 50^\circ$.

4 DISCUSSION

During the encounters not only Q’s disk is perturbed, but at the same time Q also perturbs the Sun’s disk. In particular, the preferred encounter (Tab. 1) excites the Sun’s

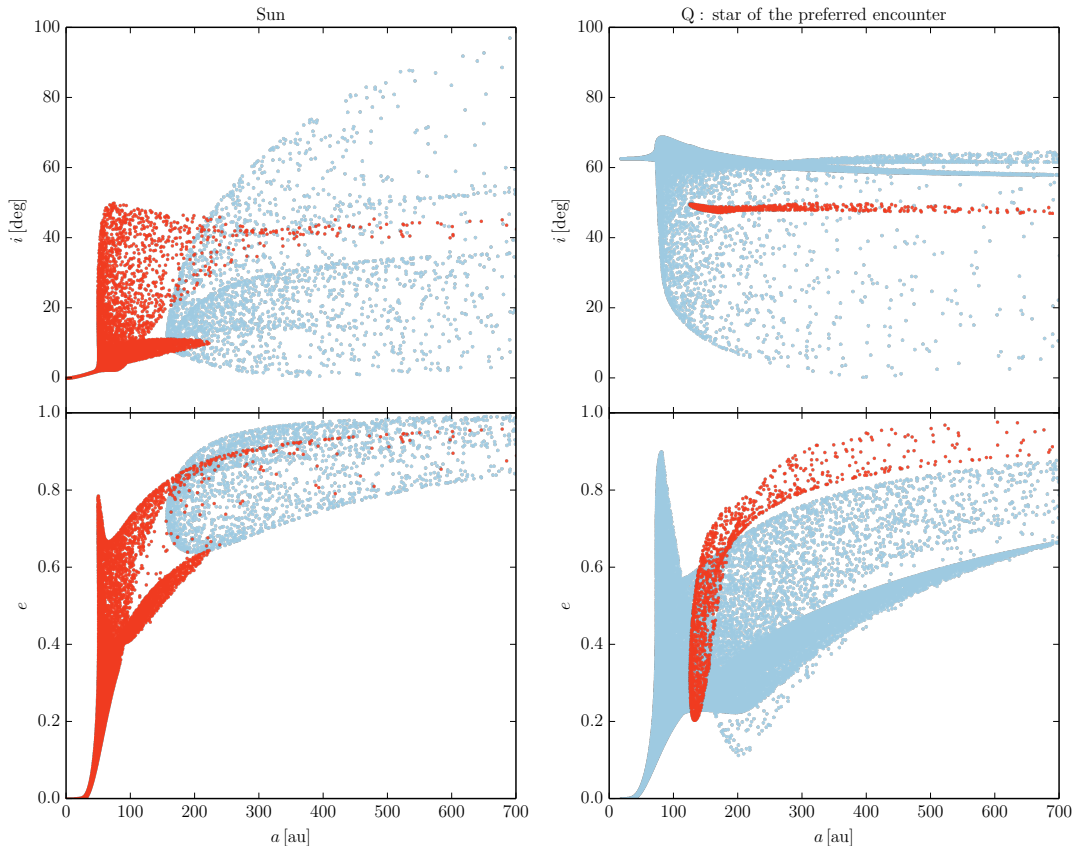


Figure 2. Orbital distributions of planetesimals for the Sun (left) and for the encountering star **Q** (right) using the preferred encounter parameters (see Tab. 1). The top panels give inclination i as a function of semi-major axis a , the bottom panels give the orbital eccentricity e . The red bullets give the orbital distributions of the planetesimals native of the Sun (assuming its disk extended to 90 au), the light blue bullets are native to the other star. Both initial planetesimal disks are strongly perturbed beyond about 30 au, but within this distance they are hardly affected (see also Kobayashi & Ida 2001). Note that the simulated particles are not weighted here.

disk beyond ~ 30 au—see left panel of Fig. 2—in agreement with the disk truncation radius estimate of Kobayashi & Ida (2001). Interestingly, the *Nice* model (Tsiganis et al. 2005; Morbidelli et al. 2005; Gomes et al. 2005) requires a truncation of the planetesimal disk at ~ 35 au (Gomes et al. 2004). Because both values are sufficiently close to be causal and a later subsequent encounter that would truncate the disk at ~ 35 au would also annihilate the population of Sednitos, the capture must have happened before the resonant planetary swap.

The observed Sednitos cluster in the argument of perihelion around $\omega = 340^\circ \pm 55^\circ$ (Trujillo & Sheppard 2014; de la Fuente Marcos & de la Fuente Marcos 2014). Such clustering is a general characteristic of an exchanged population. As discussed in Sec. 1.1, the secular evolution due to the giant planets would cause a precession of ω on timescales shorter than the age of the Solar System. If the clustering of ω is real, i.e. it is not a result of an observational bias, a mechanism preserving the distribution of ω is needed. The scenarios suggested so far involve a distant planetary-mass object (possibly more than one object) that causes libration of ω through the Kozai–Lidov mechanism (Gomes et al. 2006; Trujillo & Sheppard 2014; de la Fuente Marcos & de la Fuente Marcos 2014). Formation channels for such a super-Earth mass planet were investigated by Kenyon & Bromley

(2015), who analyzed three mechanisms: planetary migration or scattering from the inner disk (10–20 au or 5–10 au, respectively) and in-situ formation. All three mechanisms require a disk extending up to the orbit of the planet—disk of gas or small planetesimals circularizes the orbit in the former two scenarios; while the later mechanism requires a reservoir of solid material with a mass $\approx 15 M_{\text{Earth}}$ to form a planet at $a \lesssim 300$ au. However, disk and orbits of any objects beyond ~ 30 au would have been substantially perturbed by the encounters that would deposit Sednitos (see Sec. 3). The outer companion might have formed later than the Sednitos were transferred, e.g. by a capture of a free floating planet (Perets & Kouwenhoven 2012).

Understanding the origin of Sednitos and testing the theories for an outer planetary-mass object requires additional observations. The Gaia astrometric mission is expected to discover ~ 50 objects in the outer Solar System. Being a solar sibling (Portegies Zwart 2009), the encountering star may be also discovered in the coming years in the Gaia catalogues. Having been formed in the same molecular cloud, one naively expects that the chemical composition of this star is similar to that of the Sun (Brown et al. 2010). Finding back our own planetesimals in the predicted orbits around this sibling (see Fig. 2) would expose the accused robber and would put strong constraints on the extend of

the Sun's planetesimal disk. However, by now the other star has probably turned into a $\gtrsim 0.6 M_{\odot}$ carbon-oxygen white dwarf, which for a $\sim 1.8 M_{\odot}$ star happens within 2 Gyr. In that case, our stolen stones are probably lost to become free floating planetesimals due to the copious mass loss in the post-asymptotic giant branch phase of the host (Veras et al. 2011).

ACKNOWLEDGEMENTS

We thank Inti Pelupessy, Tjarda Boekholt, Adrian Hamers, and Jarle Brinchmann for enriching discussions. We thank the referee, Hal Levison, for his useful comments which helped to improve the manuscript. We thank the Leiden/ESA Astrophysics Program for Summer Students (LEAPS) for the support that made this work possible. This work was supported by the Interuniversity Attraction Poles Programme initiated by the Belgian Science Policy Office (IAP P7/08 CHARM) and by the Netherlands Research Council NWO (grants #643.200.503, #639.073.803 and #614.061.608) and by the Netherlands Research School for Astronomy (NOVA). The numerical computations were carried out using the Little Green Machine at Leiden University, and the distributed calculations were performed with the grid-version of AMUSE which was developed with support of the NLeSC.

REFERENCES

- Booth M., Kennedy G., Sibthorpe B., Matthews B. C., Wyatt M. C., Duchêne G., Kavelaars J. J., Rodriguez D., Greaves J. S., Koning A., Vican L., Rieke G. H., Su K. Y. L., Moro-Martín A., Kalas P., 2013, *MNRAS*, 428, 1263
- Brasser R., Duncan M. J., Levison H. F., 2006, *Icarus*, 184, 59
- Brasser R., Duncan M. J., Levison H. F., Schwamb M. E., Brown M. E., 2012, *Icarus*, 217, 1
- Brasser R., Schwamb M. E., 2015, *MNRAS*, 446, 3788
- Brown A. G. A., Portegies Zwart S. F., Bean J., 2010, *MNRAS*, 407, 458
- Brown M. E., Trujillo C., Rabinowitz D., 2004, *ApJ*, 617, 645
- Davies M. B., Adams F. C., Armitage P., Chambers J., Ford E., Morbidelli A., Raymond S. N., Veras D., 2014, *Protostars and Planets VI*, pp 787–808
- de la Fuente Marcos C., de la Fuente Marcos R., 2014, *MNRAS*, 443, L59
- Foreman-Mackey D., Hogg D. W., Lang D., Goodman J., 2013, *PASP*, 125, 306
- Fujii M., Iwasawa M., Funato Y., Makino J., 2007, *Publ. Astr. Soc. Japan*, 59, 1095
- Gomes R., Levison H. F., Tsiganis K., Morbidelli A., 2005, *Nat*, 435, 466
- Gomes R. S., Matese J. J., Lissauer J. J., 2006, *Icarus*, 184, 589
- Gomes R. S., Morbidelli A., Levison H. F., 2004, *Icarus*, 170, 492
- Gonçalves Ferrari G., Boekholt T., Portegies Zwart S. F., 2014, *MNRAS*, 440, 719
- Goodman J., Weare J., 2010, *Comm. App. Math. Comp. Sci.*, 5, 65
- Hastings W. K., 1970, *Biometrika*, 57, 97
- Henze N., 1988, *Ann. Statist.*, 16, 772
- Iorio L., 2014, *MNRAS*, 444, L78
- Kenyon S. J., Bromley B. C., 2004, *Nat*, 432, 598
- Kenyon S. J., Bromley B. C., 2015, *ArXiv e-prints*
- Kobayashi H., Ida S., 2001, *Icarus*, 153, 416
- Koen C., Siluyele I., 2007, *MNRAS*, 377, 1281
- Kozai Y., 1962, 67, 591
- Levison H. F., Morbidelli A., Van Laerhoven C., Gomes R., Tsiganis K., 2008, *Icarus*, 196, 258
- Lidov M. L., 1962, 9, 719
- Mardling R. A., 2007, *MNRAS*, 382, 1768
- Morbidelli A., Levison H. F., 2004, *AJ*, 128, 2564
- Morbidelli A., Levison H. F., Tsiganis K., Gomes R., 2005, *Nat*, 435, 462
- Morbidelli A., Levison H. F., Van Laerhoven C., Gomes R., Tsiganis K., 2008, in *AAS/Division of Dynamical Astronomy Meeting #39 Vol. 39 of AAS/Division of Dynamical Astronomy Meeting, Chaotic Capture of Planetesimals into Regular Regions of the Solar System. I: The Kuiper Belt*. p. 12.04
- Pak J. P., Basu A., 1998, *Ann. Statist.*, 50, 503
- Pelupessy F. I., Jänes J., Portegies Zwart S., 2012, *New Astron.*, 17, 711
- Perets H. B., Kouwenhoven M. B. N., 2012, *ApJ*, 750, 83
- Portegies Zwart S., Jilková L., 2015, *ArXiv e-prints*
- Portegies Zwart S. F., 2009, *ApJL*, 696, L13
- Portegies Zwart S. F., McMillan S. L. W., van Elteren A., Pelupessy F. I., de Vries N., 2013, *Computer Physics Communications*, 184, 456
- Punzo D., Capuzzo-Dolcetta R., Portegies Zwart S., 2014, *MNRAS*, 444, 2808
- Sussman G. J., Wisdom J., 1988, *Science*, 241, 433
- Trujillo C. A., Sheppard S. S., 2014, *Nat*, 507, 471
- Tsiganis K., Gomes R., Morbidelli A., Levison H. F., 2005, *Nat*, 435, 459
- Veras D., Wyatt M. C., Mustill A. J., Bonsor A., Eldridge J. J., 2011, *MNRAS*, 417, 2104
- Wisdom J., Holman M., 1991, *AJ*, 102, 1528